Estimating the Secondary Droplet Size Distribution after Micro-Explosion of Bio-Fuel Droplets

C. Shen, W. L. Cheng, K. Wang and C. F. Lee*
Department of Mechanical Science and Engineering
University of Illinois at Urbana-Champaign
1206 West Green Street
Urbana, Illinois 61801, USA

Abstract

Recently, some potential alternative substitutes of petroleum fuels such as biodiesel, ethanol, and butanol have received much attention because they are renewable and friendly to the environment and can possibly reduce domestic demand on foreign petroleum. Bio-fuels are generally mixed with petroleum-based diesel or gasoline in the commercial market. Since the volatilities and boiling points of ethanol/butanol and diesel/biodiesel fuels are significantly different, micro-explosion can be expected in the blend mixture. Understanding the atomization process and dynamics of secondary droplets in bio-fuel and diesel blends due to micro-explosion is helpful in optimizing bio-fuel engine performances. In this study, a numerical model of micro-explosion in multi-component bio-fuel droplets is proposed. The onset of micro-explosion is determined by the homogeneous nucleation theory and characterized by the normalized onset radius (NOR). The bubble expansion process is described by a modified Rayleigh equation. The final breakup is modeled from a surface energy approach by imposing minimal surface energy (MSE) on the system. Based on the simulated results of droplet characteristics at the onset of micro-explosion, together with the predictions from the breakup model, a simple way of estimating the Sauter mean radius (SMR) of the secondary droplets is proposed and verified against limited available experimental data. There exists an optimal droplet size for the onset of micro-explosion. It is concluded from the study that micro-explosion is possible in bio-fuel and diesel blends under engine operation conditions. The SMR of secondary droplets is estimated to be 30% to 40% of initial radius for droplets with initial radius smaller than 50 mm under micro-explosion conditions.

* Corresponding author: Chia-fon F. Lee <cflee@illinois.edu>

Introduction

The concept of micro-explosion was first presented by Ivanov in 1965 [1]. The occurrence of micro-explosion is due to the vaporization of two or more liquid components with different volatilities in a high temperature environment. Because of the finite mass diffusion velocity within the droplet, lighter components inside the multi-component droplet cannot emerge to the surface sufficiently fast to compensate its fast vaporization rate than the rest of components, and thus the mass fraction of light components inside the droplet is larger than that at the droplet surface. As a consequence, even though the droplet surface does not pass the boiling state, the temperature in some region within the droplet is likely to be higher than the local boiling point. When the temperature is high enough to support the nucleation, one or two bubbles are generated inside the droplet. Their subsequent rapid growth results in a violent explosion of the droplet [2]. The size of the secondary droplets generated by micro-explosion is decreased significantly. From the practical viewpoint, the possible occurrence of micro-explosion has potential for making fuel atomization more flexible. That is, fine atomization does not need to be the primary concern in the design of the spraying devices and processes. In fact, it may be advantageous to have somewhat larger droplet, which possess sufficient inertia to penetrate the combustor interior in order to achieve optimal charge distribution. Upon penetration rapid gasification can then be effected through micro-explosion.

Extensive experimental studies have been done to understand the vaporization and combustion behaviors of isolated droplets in micro-explosion conditions. Micro-explosion of freely falling droplets has been experimentally observed for both miscible fuel mixtures [3-5], as well as water/oil emulsions [6]. Its occurrence has also been inferred from measurements of the droplet size distribution in combusting water/oil emulsion sprays [7]. Wang and Law [4] conducted a series of micro-explosion experiments using alcohol-alkane mixtures under elevated pressures. It is reported that alcohol/diesel blends can potentially enhance atomization in diesel engine due to micro-explosion. Numerical models are proposed to describe the mechanism of micro-explosion for water in fuel emulsions [8-10]. Most studies in micro-explosion focused on the effects of pressure, composition, temperature, initial droplet size, internal phase structure of emulsified droplets and gravity on micro-explosion [4, 8-10]. Some papers studied the superheat limit, which accounts for the onset of micro-explosion [10, 11]. However, few works investigated the breakup process and the consequent outcomes before the year 2000. Based on a linear stability analysis, Zeng and Lee [2, 12] suggested a model describing the instability of micro-explosion and proposed a breakup criterion for the determination of the averaged size and velocity of secondary droplets.

Recently, some potential alternative substitutes of petroleum fuels, such as biodiesel, ethanol, and butanol, have received much attention because they are renewable and friendly to the environment [13] and can possibly reduce domestic demand on foreign petroleum. Bio-fuels are generally mixed with petroleum-based diesel or gasoline in the commercial market. Selected thermo-physical and chemical properties of ethanol, butanol, soybean biodiesel, and tetradecane are tabulated in Table 1. Since the volatilities and boiling points of ethanol and diesel/biodiesel fuels are significantly different, micro-explosion can be expected in binary mixtures of ethanol-diesel (E-D) or ethanol-biodiesel (E-B) and also in ternary mixtures of ethanol-biodiesel-diesel (E-B-D). Although butanol has a higher boiling point compared to ethanol, the differences between butanol and biodiesel are still significant so that micro-explosion in binary mixtures of butanol-biodiesel (B-B) might occur. Additionally, the use of a higher alcohol, like butanol, could solve the problem of fuel instability at low temperature because of the higher solubility of butanol in diesel/biodiesel fuels. Understanding the atomization process and dynamics of secondary droplets in bio-fuel and diesel blends due to micro-explosion is helpful in optimizing bio-fuel engine performances.

Table 1. Selected thermo-physical and chemical properties for ethanol, soybean biodiesel and tetradecane

	Ethanol	Butanol	Biodiesel	Tetradecane
Density [kg/m^3] (298 K)	789.3	810.0	885.0	759.6
Boiling Point [K]	351	400	627	527
Heat of Vaporization [kJ/kg]	841	430	320	243
Viscosity [g/cm·s] (313 K)	0.009	0.030	0.040	0.017
Surface Tension [dyne/cm] (293 K)	23.1	24.9	32.5	26.8
Vapor Pressure [mm$_{Hg}$] (353 K)	675.1	6.7	~0	2.775

In this study, the effects of ambient pressure, ambient temperature, composition, and initial droplet size on the onset of micro-explosion in bio-fuel and diesel blends are examined. Atomization is determined by the aerodynamic disturbances in previous works [2, 12]. A proposed breakup model based on surface energy of droplet is used in this study, which reaches the same results in previous works [2, 12]. The droplet breakup characteristics due to micro-explosion are studied under engine operation conditions. Numerical works are carried out by using a modified KIVA-3V Release 2 code, developed by the Los Alamos National Laboratory [14]. The thermodynamic properties of soybean biodiesel are calculated from BDProp [15] and inserted into the KIVA fuel library.

Mathematical Formulations

The proposed model describes the three crucial steps in micro-explosion of a droplet: bubble generation, bubble growth and breakup. The homogeneous nucleation theory [11] is used to calculate the generation of bubble within the droplet. After bubble generation, the modified Rayleigh equation is used to describe bubble growth [16]. Finally, the breakup process is modeled using a surface energy approach, which predicts the characteristics of the bubble and droplet at breakup. The Sauter mean radius (*SMR*) of secondary droplets after breakup can be calculated from the prediction of the breakup model. This study primarily focuses on small droplet atomization under micro-explosion and presents a simple approach to estimate the *SMR*.

Bubble Generation

Under the assumption of spherical symmetry, a bubble with radius R_b is assumed to be formed in the center of a droplet with radius R_s, according to the homogeneous nucleation theory shown in Figure 1. Zeng [12] provides the detailed thermodynamic description of the bubble-droplet system. Based on homogeneous nucleation theory, nucleation is arisen from thermal fluctuation and intermolecular interaction [17]. There is neither dissolved gas nor impurity within the bubble-droplet system acting as nucleation site. As a result, homogeneous nucleation requires a higher superheat limit [12]. Avedisian and Glassman [11] proposed a semi-empirical homogeneous nucleation rate formula shown in Eq. (1),

$$J = \Gamma\, n_0\, k_f \exp\left(-\frac{\Delta A^*}{kT}\right), \qquad (1)$$

where J (1/time-volume) is the nucleation rate; the probability of nucleation; n_0, the number density; k_f, the gas collision frequency; and A^* is the activation energy. The mathematical descriptions of parameters in Eq. (1) can be found in [11]. The current work uses unity for as in previous studies [2, 11, 12, 18], which allows accurate prediction, relative to experimental measurements of the superheat limit.

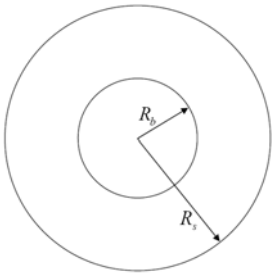

Figure 1. Bubble-droplet system

The number of nuclei can be calculated by integrating Eq. (1) with respect to time over the control volume [2]. The onset of micro-explosion, which signifies the instant of bubble generation, is determined by setting the number of nuclei to one. The exponential form on the nucleation rate indicates the drastic growth of the number of nuclei once the droplet temperature approaches the superheat limit. Therefore, the choice of the number of nuclei is insignificant in the determination of the onset of micro-explosion.

The primary concern of using homogeneous nucleation theory is that heterogeneous nucleation, due to the existence of impurity or dissolved gas, is likely to take place in practice. However, the temperature at which heterogeneous nucleation happens is bounded by the superheat limit and the saturation temperature [19, 20]. In other words, heterogeneous nucleation is possible if the droplet temperature is between these two limits. At high ambient pressure, the superheat limit and the saturation temperature approach each other [2, 11, 12, 18]. This justifies the use of homogeneous nucleation theory in determining the nucleation temperature at high ambient pressure.

After bubble generation, the initial radius of the bubble nucleus is given by the Young-Laplace equation,

$$R_b^* = \frac{2\sigma}{P_g - P_l}, \qquad (2)$$

where σ is the surface tension, P_g is the gas pressure in the bubble, P_l is the liquid droplet pressure, and R_b^* is the initial radius of the bubble. Eq. (2) addresses the mechanical equilibrium between the bubble and liquid droplet [16].

Bubble Growth

The modified Rayleigh equation describes the bubble growth process [16, 21],

$$\rho_l\left[R_b\frac{d^2R_b}{dt^2}+1.5\left(\frac{dR_b}{dt}\right)^2\right]=P_g-P_l-\frac{2\sigma}{R_b}, \quad (3)$$

where ρ_l is the liquid droplet density. The above equation states that pressure work across the gaseous-liquid interface ($r = R_b$ in Figure 1) is converted into kinetic energy, the two terms on the left hand side and surface energy, the last term on the right hand side. Note that dR_b/dt is the bubble expansion velocity. Some studies add viscous terms into the Rayleigh equation to account for the viscous effect during bubble expansion. Robinson and Judd [16] showed that viscous effect is negligible compared to other terms throughout the parameter space in that study. Eq. (3) is derived by assuming the bubble expanding in an infinite medium and thus excludes the finite size effect of the medium. Additional works will be needed to extend Eq. (3) for a finite medium. In this study, the modified Rayleigh equation is mainly used to characterize the bubble expansion rate. It also gives the estimation of the Weber number at droplet surface in a small bubble-droplet system.

Sauter Mean Radius of Secondary Droplets

Consider a bubble-droplet system with bubble radius R_b, droplet surface radius R_s, and bubble expansion rate (V_b), written as dR_b/dt in Eq. (3), at the instant of breakup; the SMR of the secondary droplets can be obtained from conservation equations, assuming the system is spherical symmetric as in [18]. Previous work [12] assumes the secondary droplets are Chi-squared (χ^2) distributed. Current model extends previous derivation [12] by describing the size distribution of the secondary droplets using a generic probability distribution. Replacing the bubble expansion rate V_b by droplet surface expansion rate V_s in the conservation of mass and rewrite the SMR equation in terms of void fraction, $\varepsilon = R_b^3 / R_s^3$, ($0 \le \varepsilon <$ 1 in bubble-droplet system), and surface Weber number, $We_s = \rho_l R_s V_s^2$, the SMR equation then becomes:

$$SMR^{-1}=\frac{1}{R_s}\left\{\frac{1+\varepsilon^{2/3}}{1-\varepsilon}+\left[\frac{1}{2}\frac{\varepsilon^{-1/3}-1}{1-\varepsilon}-\frac{3}{2}\left(\frac{1-\varepsilon^{1/3}}{1-\varepsilon}\right)^2\right]We_s\right\} \quad (4)$$

Note that R_s, ε, and We_s in Eq. (4) are unknowns. Assuming that liquid mass is approximately conserved during bubble expansion, $R_{s0}^3 \approx R_s^3 - R_b^3$, droplet surface radius, R_s, can then be expressed in terms of the droplet radius right before the onset of micro-explosion, R_{s0}, and void fraction ε,

$$R_s=\frac{R_{s0}}{(1-\varepsilon)^{1/3}}, \quad (5)$$

where R_{s0} refers to droplet surface radius at $\varepsilon = 0$. Since the initial radius of bubble at the onset of micro-explosion is much smaller than droplet size [2], i.e. $\varepsilon \approx 0$, R_{s0} can also be regarded as the droplet surface radius at the onset of micro-explosion. Since the time elapsed between bubble generation and droplet breakup is fairly small relative to droplet lifetime, the assumption of liquid mass conservation during bubble growth can be made [12]. Substituting Eq. (5) into (4), the SMR equation becomes:

$$SMR^{-1}=\frac{(1-\varepsilon)^{1/3}}{R_{s0}}\left\{\frac{1+\varepsilon^{2/3}}{1-\varepsilon}+\left[\frac{1}{2}\frac{\varepsilon^{-1/3}-1}{1-\varepsilon}-\frac{3}{2}\left(\frac{1-\varepsilon^{1/3}}{1-\varepsilon}\right)^2\right]We_s\right\}. \quad (6)$$

Once R_{s0} is known and ε and We_s are determined, the *SMR* can then be estimated.

Breakup Criterion: Minimal Surface Energy (MSE)

A breakup model is derived to determine the onset of micro-explosion. The key concept of this breakup model is the surface energy, which will be shown proportional to Gibbs free energy, of the bubble-droplet system by assuming breakup takes place at some unknown ε and We_s. Then the minimal surface energy (MSE) in the ε and We_s domains are used to determine the most probable ε and We_s for breakup.

To relate the Gibbs free energy and surface energy using a thermodynamic relation between, assuming constant surface tension and mass, and the system remains isothermal and quasi-steady within a differential expansion. The differential form of Gibbs free energy of the bubble-droplet system takes the following form, assuming negligible temperature change,

$$dG = V\,dP + \sigma\,dA, \quad (7)$$

where

$$V\,dP=\frac{4}{3}\pi R_b^3\,dP_g+\frac{4}{3}\pi\left(R_s^3-R_b^3\right)dP_l, \quad (8)$$

and

$$\sigma\,dA = 4\pi\sigma\,d\left(R_b^3+R_s^3\right). \quad (9)$$

Under quasi-steady state assumption, dP_l and dP_g can be obtained from the Young-Laplace equation at R_s and R_b. Finally, dG can be expressed by

$$dG=\frac{2}{3}\sigma\,dA. \quad (10)$$

The Young-Laplace equation considers mechanical equilibrium across the gas-liquid interface, which is an

appropriate approximation for a small bubble-droplet system under high ambient pressure where the pressure and surface forces are the dominate terms during bubble expansion. The isothermal assumption is usually good because the droplet temperature is nearly constant within the differential expansion if the ambient temperature is constant. Eq. (10) shows that the surface energy of the system is proportional to Gibbs free energy. In other words, the system attains the minimum of Gibbs free energy as long as the minimum of surface energy is achieved.

The initial surface energy, SE_0, of the system right before the onset of micro-explosion (at $\varepsilon = 0$) is

$$SE_0 = 4\pi R_{s0}^2 \sigma . \quad (11)$$

The surface energy of the system at some ε before breakup is

$$SE_1 = 4\pi R_s^2 \left(1 + \varepsilon^{2/3}\right) \sigma = 4\pi R_{s0}^2 \frac{1 + \varepsilon^{2/3}}{(1 - \varepsilon)^{2/3}} \sigma . \quad (12)$$

To describe the surface energy of the system immediately after breakup at some ε and We_s, assume the secondary droplets obey a separable and spherically symmetric probability distribution function,

$$f = f(r, \theta, \varphi) = f_r(r) f_\theta(\theta) f_\varphi(\varphi) . \quad (13)$$

Then the total surface energy after breakup becomes

$$SE_2 = N \int \int 4\pi r^2 \sigma f_r(r) f_\theta(\theta) f_\varphi(\varphi)\, dr\, d\theta\, d\varphi = 4\pi \sigma N \int r^2 f_r\, dr \quad (14)$$

where N is the number of secondary droplets and r denotes the radius of a secondary droplet. The mass conservation gives:

$$\frac{4\pi}{3} \rho_l \left(R_s^3 - R_b^3\right) = \int N \frac{4\pi}{3} \rho_l r^3 f_r(r)\, dr . \quad (15)$$

To rewrite SE_2 in the form of Eq. (12), divide Eq. (14) by (15) and substitute Eq. (6) for *SMR*, defined as

$$\int r^3 f_r(r)\, dr \Big/ \int r^2 f_r(r)\, dr . \quad (16)$$

To compare the surface energy at various ε and We_s, normalize Eqs. (12) and (16) by (11), gives:

$$\frac{SE_1}{SE_0} = \frac{1 + \varepsilon^{2/3}}{(1 - \varepsilon)^{2/3}} , \quad (17)$$

$$\frac{SE_2}{SE_0} = \frac{1 - \varepsilon}{(1 - \varepsilon)^{2/3}} \left\{ \frac{1 + \varepsilon^{2/3}}{1 - \varepsilon} + \left[\frac{1}{2} \frac{\varepsilon^{-1/3} - 1}{1 - \varepsilon} - \frac{3}{2} \left(\frac{1 - \varepsilon^{1/3}}{1 - \varepsilon} \right)^2 \right] We_s \right\} . \quad (18)$$

Eq. (17) presents a non-dimensional form of surface energy as a function of void fraction if there is no breakup; while Eq. (18) depicts the minimal surface energy ratio if breakup takes places at some void fraction, ε, and Weber number, We_s. Eq. (17) is a monotonically increasing function in SE_1/SE_0 with respect to ε; while Eq. (18) has minimum values in SE_2/SE_0 over the ε and We_s domains. The ε and We_s which produce minimal SE_2/SE_0 are referred to the possible void fraction and Weber number for breakup in this work. The SMR for the secondary droplets can then be estimated by substituting the ε and We_s that produce the minimal SE_2/SE_0 into Eq. (6). The result from the MSE approach is the same as the results by Zeng and Lee [2, 12], where atomization is determined by the aerodynamic disturbances.

Results and Discussion

A numerical study is conducted to exam the effects of ambient pressure, ambient temperature, and composition of the mixture on the onset of micro-explosion. The effect of biodiesel on micro-explosion is then studied by comparing the results for ethanol-tetradecane and ethanol-biodiesel-tetradecane droplets. The onset of micro-explosion is referred as bubble generation, which is a prerequisite of micro-explosion. The droplet size decreases upon evaporation while the nucleation process is initiated. Therefore, micro-explosion can be characterized by the normalized onset radius (NOR), the ratio of droplet radius at the onset of micro-explosion to the initial droplet radius, assuming that the time elapsed between the onset and final breakup of the droplet is negligible relative to the droplet lifetime [16]. The NOR represents the possibility of micro-explosion: a large NOR implies that micro-explosion is more likely to take place and vice versa. Based on the spherical symmetry assumption, the bubble-droplet system is simplified to a one-dimensional problem.

Effects of Ambient Pressure

A set of calculations is done on ethanol-tetradecane (E-D), butanol-biodiesel (B-B), and ethanol-biodiesel-tetradecane (E-B-D) droplets at different ambient pressures. The initial droplet radius is 300 μm and the initial liquid temperature is 300 K. Ambient temperature is assumed to be 2300 K, which is about the adiabatic flame temperature for typical hydrocarbons.

Figure 2 shows the NOR for a 50% ethanol-50% tetradecane droplet, and a 30% ethanol-20% biodiesel-50% diesel droplet. The slope of the curve decreases as pressure increases and eventually becomes negative at very high pressure. The maximum NOR occurs at about 24 atm for the 50% ethanol-50% tetradecane droplet and 26 atm for the 30% ethanol-20% biodiesel-50%

diesel droplet. Model predictions are consistent with experimental measurements [4]. Bubble nucleation is suppressed at ambient pressures higher than 28 atm [11]. The figure also shows that adding biodiesel into ethanol-diesel blends enhances the possibility of micro-explosion because added biodiesel enlarges the difference in boiling points and volatilities (Table 1) that stimulates micro-explosion.

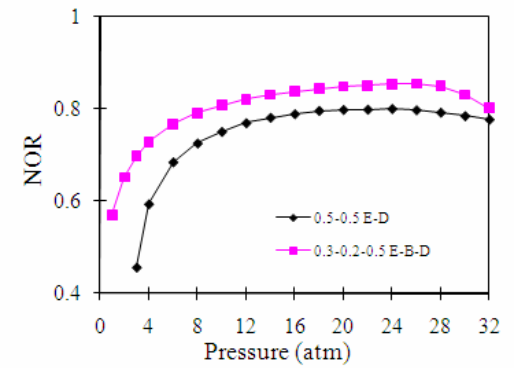

Figure 2. The effects of ambient pressure on micro-explosion for ethanol-tetradecane (E-D) and ethanol-biodiesel-tetradecane (E-B-D) droplets

Figure 3 shows the NOR for a 20% butanol-80% biodiesel droplet. Same as shown in Figure 2, a peak point of the NOR was observed. With increasing pressure, the required superheat degree for homogeneous nucleation decreases, which favors homogenous nucleation. On the other hand, the volatility difference between components decreases, which suppresses nucleation. Compared to the ethanol blends, the maximum NOR for butanol blends occurs at a lower pressure, which is about 11 atm.

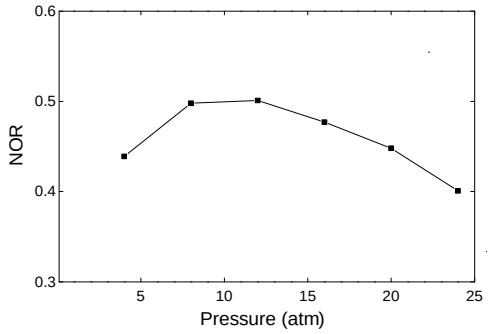

Figure 3. The effects of ambient pressure on micro-explosion for 20% butanol-80% biodiesel (B-B) droplet

Effects of Ambient Temperature

Figure 4 shows the effect of ambient temperature on the onset of micro-explosion for a 50% ethanol-50% tetradecane droplet, and a 50% ethanol-20% biodiesel-30% diesel droplet with a fixed ambient pressure 10 atm. With ambient temperature varying from 1000 K to 2200 K, there is no noticeable effect on the NOR. This indicates that varying the ambient temperature will not alter the possibility of micro-explosion for ethanol blend. However, it is possible that adding into the blend may stimulate micro-explosion, because biodiesel is more non-volatile than diesel, and it is easier for ethanol to reach the superheat limit by adding more biodiesel.

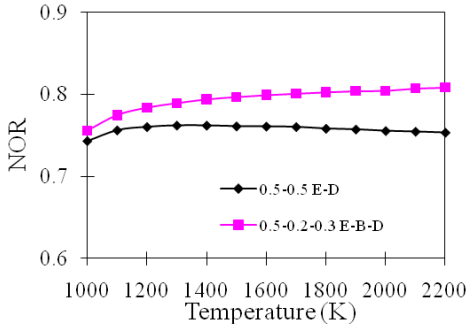

Figure 4. The effects of ambient temperature on micro-explosion for ethanol-tetradecane (E-D) and ethanol-biodiesel-tetradecane (E-B-D) droplets

The effect of ambient temperature on the onset of micro-explosion for butanol-biodiesel mixture is quite obvious as shown in Figure 5. The ambient pressure is fixed at 20 atm, and the fuel droplet is composed by 20% butanol-80% biodiesel. When ambient temperature is increased from 1000 K to 2300 K, the NOR is decreased by about 40%. This may be because the evaporation is stronger for higher ambient temperature, which ends up with smaller NOR. No micro-explosion is observed during the droplet lifetime with ambient temperature less than 1000 K. It indicates that if the ambient temperature is too low, the heat transfer rate will not be fast enough for the droplet to reach the superheat limit.

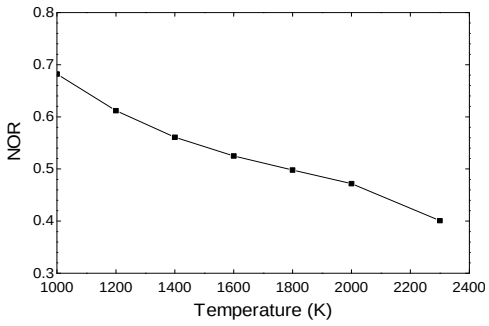

Figure 5. The effects of ambient temperature on micro-explosion for 20% butanol-80% biodiesel droplet

Effects of Composition

Figure 6 shows the effect of composition of ethanol-tetradecane, ethanol-biodiesel and ethanol-20% biodiesel-tetradecane droplets with initial radius of 300 μm. The optimum composition for the ethanol-tetradecane droplet is located at approximately equal composition. Adding biodiesel to the ethanol-tetradecane mixture enhances the possibility of micro-explosion, at any given mass fraction of ethanol. For the ethanol-biodiesel droplet, the optimal composition for micro-explosion is 30% ethanol and 70% biodiesel. The NOR is about 92%. As the amount of biodiesel increases, the maximum NOR shifts towards a lean mixture, implying micro-explosion is caused by high superheat. From Table 1, adding biodiesel to an ethanol-tetradecane mixture increases the difference in volatility and boiling point among the components. The enlarged difference changed the amount of superheat that ethanol, the most volatile component, encounters during the evaporation of the droplet, which shifts the optimal composition as shown in Figure 6.

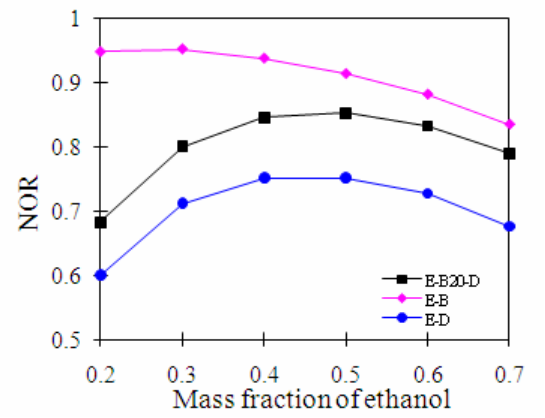

Figure 6. The effects of composition on ethanol-tetradecane (E-D), ethanol-biodiesel-tetradecane (E-B-D) and ethanol-biodidsel (E-B) droplets, initial radius of 300 μm

Figure 7 shows the effect of composition of butanol-biodiesel droplet with the same initial radius as in Figure 6. The optimum composition is 30% butanol-70% biodiesel, which is the same optimum composition for ethanol-biodiesel blends. No micro-explosion is observed for butanol-diesel blends with butanol composition varying from 20% to 80%. As shown in Table 1, the boiling point of butanol is higher than ethanol, so the difference in volatility and boiling point between butanol and diesel may not be significant enough to support homogeneous nucleation. Therefore, the occurrence of micro-explosion in butanol-diesel mixture is more difficult. Because biodiesel has a higher boiling point than diesel, micro-explosion in butanol-biodiesel blends is observed.

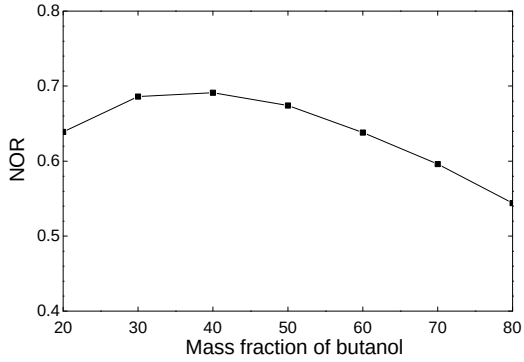

Figure 7. The effects of composition on butanol-biodiesel droplet, initial radius of 300 μm

Effects of Initial Droplet Size

Figure 8 shows the effect of size on the onset of micro-explosion of a 50% ethanol-50% tetradecane droplet. The ambient pressure and temperature are 40 atm and 825 K, respectively, which are similar to typical conditions in diesel engine operations.

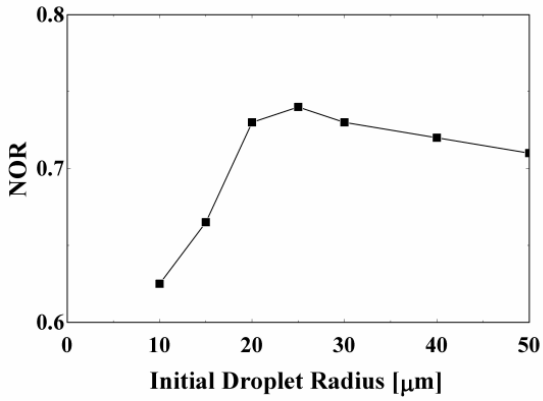

Figure 8. The NOR of 50% ethanol – 50% tetradecane mixtures

Figure 8 shows an initial radius of about 25 μm being the optimal size for micro-explosion, which has a NOR of 0.725. The surface to volume ratio is larger for small droplet, resulting in stronger evaporation during the heat up process, which ends up with smaller NOR. No micro-explosion is observed during the droplet lifetime for droplets with initial radius less than 10 μm. For droplets with initial radius larger than 25 μm, the NOR reduces slightly with larger initial radius. This may due to the fact that a larger droplet requires more heat transfer from the environment to achieve its superheat limit and thus it takes longer for bubble generation, which results in a smaller NOR. These

results show that micro-explosion is possible for small droplets under engine environments.

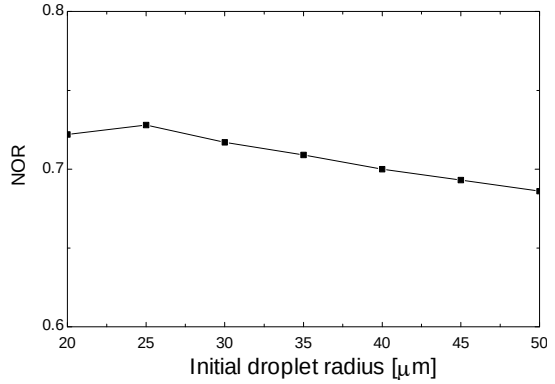

Figure 9. The NOR of 20% butanol – 80% biodiesel mixtures

Figure 9 shows the effect of size on the onset of micro-explosion of a 20% butanol-80% biodiesel droplet. The ambient pressure and temperature are 20 atm and 1200 K, respectively. Similar to ethanol-diesel blends, Figure 9 shows that the optimal initial droplet radius for micro-explosion of butanol-biodiesel blends is also about 25 μm, which has a NOR of 0.728. For droplets with initial radius less than 20 μm, no micro-explosion is observed during the droplet lifetime. The minimal droplet size for micro-explosion of butanol blends is higher than ethanol blends. This may due to the fact that butanol has a higher boiling point, and it needs longer time for internal gasification. Therefore, small droplet will vanish due to evaporation before micro-explosion occurs. These results also show that micro-explosion is also possible for butanol-biodiesel fuel blends under engine environments.

Micro-Explosion and the Sauter Mean Radius of Secondary Droplets

From the simulation results of Eq. (3), We_s is about of O(10) for droplets with initial radius ranges from 10 μm to 50 μm and the aforementioned ambient conditions. Generally speaking, larger droplets tend to reach higher We_s during bubble expansion because of the larger dimension. To decide the possible ε upon breakup at any given We_s, the non-dimensional minimal surface energy after breakup, SE_2/SE_0, in Eq. (18) or simply called minimal surface energy ratio (*MSER*) hereafter, is plotted against ε and We_s, as shown in Figure 10.

It can be seen from Figure 10 that *MSER* reaches high values at both small and large ε, which means neither small nor large ε is favorable for droplet breakup. However, it should be noted that at very small We_s, like the simulated cases in this study, the *MSER* can occur at small ε, which is not intuitive according to conventional concept. As far as a small droplet is considered, a small ε still ends up with a small droplet thickness, which equals to $R_s - R_b$, due to its small R_s, which provides a reasonable explanation of the small ε upon breakup for a small droplet.

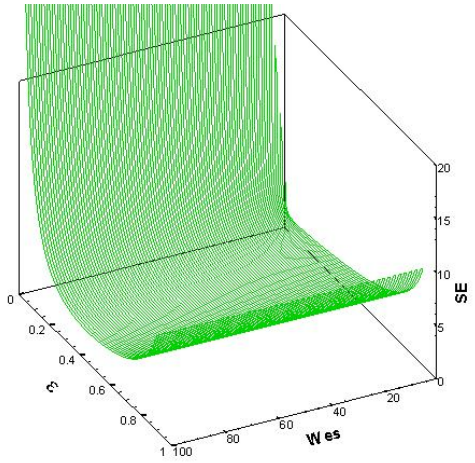

Figure 10. The minimal surface energy ratio (SE_2/SE_0, or MSER) if breakup takes place at some ε and We_s

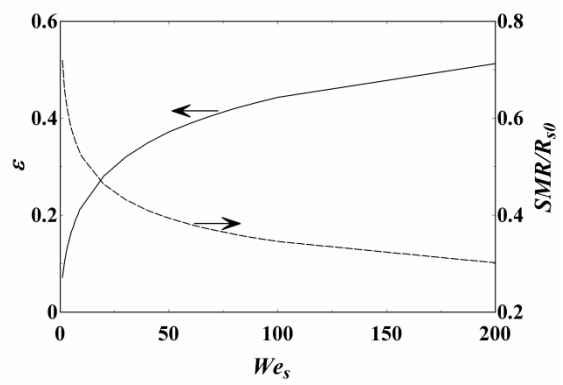

Figure 11. The possible ε at breakup and the corresponding We_s and SMR/R_{s0}

Figure 11 shows ε and the corresponding We_s and SMR/R_{s0} at the *MSER* in Figure 10. SMR/R_{s0} is calculated from Eq. (6) by substituting possible ε and We_s at breakup. At We_s of 10, the possible ε at breakup is 0.218. As We_s increases to 200, referring to a large droplet case, the possible ε at breakup becomes 0.513, which is similar to the measurements in fuel jet breakup experiment by Suma and Koizumi [23] and the empirical breakup model in flash boiling by Kawano et al [24]. Suma and Koizumi's experimental data of ε at breakup range from 0.51 to 0.53. It is interesting to point out that, further reduction in the SMR is possible if We_s increases, as shown in Figure 10. This shows that

micro-explosion may be more effective in atomizing large droplets. Further examinations are needed to characterize micro-explosion phenomenon in large droplets, current work focused only on small droplets.

For the $We_s = 10$ case, it can be referred from Figure 10 that the SMR is 52% of the droplet radius at the onset of micro-explosion. From Figure 8, for 0.5-0.5 E-D droplets with initial radius ranging from 20 μm to 50 μm, the droplet radius at the onset of micro-explosion is about 72% of initial radius. Therefore, the SMR of the secondary droplets is approximately 37% of the initial radius. Figure 11 presents a simple approach in estimating the SMR of secondary droplets as long as the radius at the onset of micro-explosion is known and it is possible to estimate the Weber number.

Conclusion

The KIVA-3V Release 2 code is used to study micro-explosion in droplets composed of blends of bio-fuel and diesel. A breakup model is derived using the minimal surface energy (MSE) approach. Based on the breakup model, a simple way of estimating the Sauter mean radius of the secondary droplets is proposed and verified against limited available experimental data. The effects of mixture composition, ambient temperature and pressure, and initial droplet size on micro-explosion are examined in this study. Then, the simulated results of droplet characteristics at the onset of micro-explosion, together with the predictions from the breakup model, are used to estimate the Sauter mean radius after breakup. From the results, the following conclusions can be made:

(1) Micro-explosion, characterized by the normalized onset radius (NOR), is possible in bio-fuel and diesel blends under engine operation conditions.

(2) The optimum initial radius of a binary droplet composed of 50% ethanol and 50% tetradecane, under typical engine condition (ambient temperature and pressure of 825 K and 40 atm, respectively), for the onset of micro-explosion is approximately 25 μm.

(3) The ambient temperature does not have noticeable effects on the occurrence of micro-explosion for ethanol-diesel and ethanol-biodiesel-diesel blends. However, for butanol-biodiesel blends, lower temperature will stimulate micro-explosion.

(4) Increasing ambient pressure favors micro-explosion under low pressure condition. On the other hand, further increasing pressure will suppress micro-explosion.

(5) Adding biodiesel, less volatile than ethanol and diesel, into the ethanol-tetradecane mixture can improve the possibility of micro-explosion. Also, micro-explosion is observed in a binary droplet of butanol-biodiesel.

(6) The SMR of secondary droplets is estimated to be 30% to 40% of initial radius for droplets with initial radius smaller than 50 μm under micro-explosion conditions.

(7) The MSE approach reaches the same conclusion as the model developed by Zeng and Lee [2, 12], where atomization is determined by the aerodynamic disturbances.

(8) The SMR of secondary droplets can be estimated by the possible ε at breakup and the corresponding We_s and SMR/R_{s0} at the minimal surface energy ratio (MSER), see Figure 11, generated from results of the current model based on MSE approach.

The current work uses a modified Rayleigh equation which accounts for bubble expansion in an infinite medium to calculate the surface Weber number. For better predictions of the Weber number, finite size effect must be considered in the Rayleigh equation. Future experimental measurements of bubble expansion and secondary droplet size are needed to verify the present breakup model.

Acknowledgements

This work was supported in part by the Department of Energy Grant No. DE-FC26-05NT42634, and by Department of Energy GATE Centers of Excellence Grant No. DE-FG26-05NT42622.

References

[1] V. M. Ivanov and P. I. Nefdov, NASA TT F-258 (1965).

[2] Y. Zeng, C. F. Lee, *Proceedings of the Combustion Institute.* 31 (2007) 2185-2193.

[3] J. C. Lasheras, A. C. Fernandez-Pello, F. L. Dryer, *Combust. Sci. Tech.* 22 (1980) 195-209.

[4] C. H. Wang and C. K. Law, Combustion and Flame 59 (1985) 53-62.

[5] J. C. Lasheras, A. C. Fernandez-Pello, F. L. Dryer, *Eighteenth Symposium (International) on Combustion.* The Combustion Institute, Pittsburgh, 1981, 293-305.

[6] J. C. Lasheras, A. C. Fernandez-Pello, F. L. Dryer, *Combust. Sci. Tech.* 21 (1979) l-4.

[7] Y. Mizutani, A. Taki, *ASME* paper 80-WA/HT-36 (1980).

[8] W. B. Fu, L. Y. Hou, L. Wang and F. H. Ma, Fuel Proceeding Tech. 79 (2002) 107-119.

[9] K. C. Tsao and C. L. Wang, SAE Paper No. 860304, Warrendale, PA (1986).

[10] C. K. Law, Combustion Science and Tech. 17 (1977) 29-38.

[11] C. T. Avedisian and I. Glassman, ASME J. Heat Transfer 103 (1981) 272-280.

[12] Y. Zeng, Ph.D. Thesis, University of Illinois, Mechanical Engineering (2000).

[13] X. Pang, X. Shi, Y. Mu, H. He, S. Shuai, H. Chen and R. Li, Atmospheric Environment 40 (2006) 7057-7065.

[14] A. Amsden, KIVA-3V: a Block-Structured KIVA Program for Engines with Vertical or Canted Valves, Los Alamos Natl. Lab. Rep. LA-13313-MS (1997).

[15] W. Yuan, Ph.D. Thesis, University of Illinois, Agricultural Engineering (2005).

[16] Robinson, A.J. and Judd, R.L., Int. J. Heat Mass Transfer 47: 5101-5113 (2004).
[17] V. P. Skripov, Metastable Liquids, Translated from Russian by R. Kondor, Wiley, New York (1974).
[18] C. F. Lee, K. T. Wang and W. L. Cheng, SAE Paper 2008-01-0937 (2008).
[19] E. Gerum, J. Straub U. and Grigull, Int. J. Heat Mass Transfer 22 (1979) 517-524.
[20] M. Blander and J. L. Katz, AIChE Journal 21 (1975) 833-848.
[21] L. E. Scriven, Chemical Engineering Science 12 (1960) 98-108.
[22] C. T. Avedisian, Proceedings of the Royal Society of London, Series A: Mathematical and Physical Sciences, 409 (1987) 271-285.
[23] S. Suma and M. Koizumi, Trans. JSME (B) 43 (1977) 4608-4617.
[24] D. Kawano, H. Ishii, H. Suzuki, Y. Goto, M. Odaka and J. Senda, Heat Transfer-Asian Research, 35 (2006) 369-385.